Proceedings of the ASME 2013 International Design Engineering Technical Conferences &
Computers and Information in Engineering Conference
IDETC/CIE 2013
August 4-7, 2013, Portland, Oregon, USA

DETC2013-13004

SOFT PNEUMATIC ARTIFICIAL MUSCLES WITH LOW THRESHOLD PRESSURES FOR A CARDIAC COMPRESSION DEVICE

Steven C. Obiajulu
Department of Mechanical Engineering
Massachusetts Institute of Technology
Cambridge, MA, USA

Ellen T. Roche
Wyss Institute for Biologically Inspired Engineering
School of Engineering and Applied Sciences
Harvard University
Cambridge, MA, USA

Frank A. Pigula, M.D.
Department of Cardiac Surgery
Children's Hospital Boston
Boston, MA, USA

Conor J. Walsh, Ph. D
Wyss Institute for Biologically Inspired Engineering
School of Engineering and Applied Sciences
Harvard University
Cambridge, MA, USA

ABSTRACT

In this paper, we present the design, fabrication and characterization of fully soft pneumatic artificial muscles (PAMs) with low threshold pressures that are intended for direct cardiac compression (DCC). McKibben type PAMs typically have a threshold pressure of at least 100 kPa and require rigid end fittings which may damage soft tissue and cause local stress concentrations, and thus failure points in the actuator. The actuator design we present is a variant on the McKibben PAM with the following key differences: the nylon mesh is embedded in the elastomeric tube, and closure of the end of the tube is achieved without rigid ends. The actuators were tested to investigate the effects of mesh geometry and elastomer material on force output, contraction, and rise time. Lower initial mean braid angles and softer elastomer materials provided the best force, contraction, and rise times; Up to 50 N of force, 24% contraction, and response times of 0.05 s were achieved at 100 kPa. The actuators exhibited low threshold pressures (<5 kPa) and high rupture pressures (138 kPa – 720 kPa) which suggest safe operation for the DCC application. These results demonstrate that the actuators can achieve forces, displacements, and rise times suitable to assist with cardiac function.

INTRODUCTION

Pneumatic artificial muscles (PAMs) are actuators that contract when pressurized with air. The most widely used PAM is the Mckibben PAM [1]. This tube-like actuator was developed in the 1950s for actuating orthotics because of the similarity between its load-length curve and that of skeletal muscle. McKibben PAMs consist of a rubber tube enclosed in a textile mesh or braid. The mesh contracts axially when the bladder expands it radially, acting in a manner similar to a scissor linkage. At their ends, the bladder and mesh are crimped together to allow mechanical coupling to a load.

McKibben PAMs have been used in a wide range of applications including robotics, orthotics, and industrial automation [2]. One potential new application that we are proposing is in direct cardiac compression (DCC), a treatment for end-stage heart failure. DCC involves implantation of a device that surrounds the heart and contracts in phase with the native heartbeat to provide direct mechanical assistance during the ejection phase (systole) of the cardiac cycle. Unlike other treatment options, DCC does not require contact with the patient's circulating blood. This is advantageous because blood-contacting devices are associated with thromboembolic events, hemolysis, immune reactions and infections [3]. DCC devices are typically implanted through open heart surgery and are usually powered through a transcutaneous drive line. A number

of actuation strategies for DCC have been implemented, pneumatic and otherwise [4–11]. To date it seems that McKibben PAMs have been ignored as an actuation strategy. If integrated into DCC devices, McKibben PAMs may provide more physiological and atraumatic actuation because they have load-length curves similar to human muscle [12,13] and are self-limiting.

Unfortunately, traditional McKibben PAMs have properties that could limit their use inside the human body. The foremost drawback is that McKibben PAMs typically have a threshold pressure of 100kPa due to friction between the bladder and mesh coupled with an initial lack of contact between the walls of the bladder and mesh. This limitation prevents precise control of force and displacement Low forces and controlled displacements cannot be achieved with PAMs that have high threshold pressures because there is a rapid jump in force and displacement as the threshold is passed [1]. This may be traumatic to the heart after many cycles. Besides that effect, a higher threshold pressure would require a higher operating pressure, but it is unsafe to have high pressures inside the body in case the device ruptures. Finally, a high threshold pressure introduces a delay since the actuator cannot begin delivering power until the threshold is passed.

Additionally, most existing McKibben PAMs have rigid attachment points at their ends that allow for easy mechanical coupling to a load. If McKibben PAMs were used for DCC, such features might damage a patient's soft tissue. Also, the crimps have been shown to cause early fatigue failure due to introduction of stress concentrations [1,14].

In the present study, a new variant of the McKibben PAM that integrates the braid with an elastomeric tube was designed to be compatible with DCC. The PAMs were designed with a low threshold pressure and soft ends. The PAMs were evaluated to assess whether they provided suitable force, contraction, and rise times for DCC and to evaluate how output force and contraction were affected by changes to elastomeric material and braid angle.

DESIGN OF PNEUMATIC ARTIFICIAL MUSCLES

Overview of Pneumatic Artificial Muscles

The force produced by a PAM depends on its internal pressure and its contraction, but not its initial length. Force increases linearly with increasing internal pressure and decreases with increasing contraction, thus at least two sets of tests are required to characterize the force output of the muscle. Using energy conservation, an expression for the force output of a PAM can be derived:

$$F = -P\frac{dV}{dl}. \tag{1}$$

F is output force, P is input pressure, dV is change in the actuator's internal volume and dl is the change in the actuator length. Assuming a thin wall and neglecting friction and effects

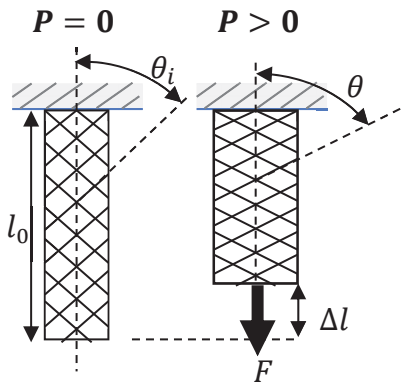

Figure 1. DEFINITION OF PARAMETERS.

of bladder elasticity, Schulte [15] showed that for a McKibben PAM

$$F = P \cdot \frac{\pi D_0^2}{4}(3\cos^2\theta - 1), \tag{2}$$

where θ is the braid angle (assumed to be uniform) and D_0 is the diameter of the mesh at a braid angle of 90 degrees. The relevant parameters are defined in Fig. 1.

The contraction, ϵ of a PAM is defined as

$$\epsilon = \frac{l_0 - l}{l_0}, \tag{3}$$

where l is length and l_0 is initial length. Using a simple geometric model of the McKibben PAM, ϵ can be related to the braid angle of the mesh by the equation [16]

$$\epsilon = 1 - \frac{\cos(\theta)}{\cos(\theta_0)}. \tag{4}$$

In the above equation, the initial braid angle, θ_0, is a constant determined by the braid pattern used to construct a PAM. Increasing pressure drives the braid angle asymptotically to θ_{max} = 54.7° because internal volume is maximized at this angle [16,17]. Since increasing pressure drives θ to θ_{max} and θ_0 is assumed to be fixed for a PAM, Eqn. 4 implies that increasing pressure drives contraction to a constant value. One implication of this result is that the capacity for contraction can be increased only by lowering θ_0.

Another implication is that if $\theta_0 = \theta_{max}$, no axial contraction occurs. For all PAMs, radial expansion accompanies axial contraction, but radial expansion of the ends of the actuator can cause the air supply line to be ejected. To prevent this from happening, rigid end fittings are typically used to secure the air supply line. In the PAMs developed here, instead of using rigid ends fittings, θ_0 was locally set close to θ_{max} at the ends of the mesh to prevent radial expansion there. Since the braid angle was only modified over a small length of

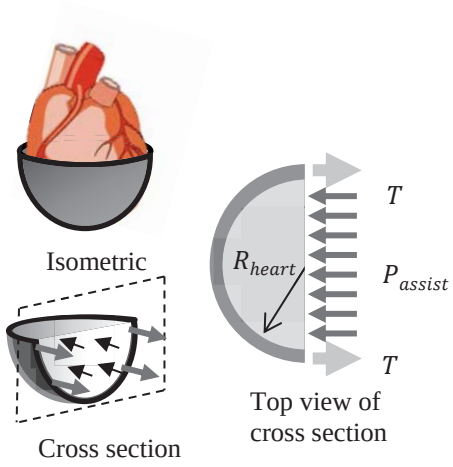

Figure 2. AN IDEALIZED MODEL OF A CUP-SHAPED DCC DEVICE THAT SITS OVER THE APEX OF THE HEART AND A FREE BODY DIAGRAM OF HALF OF THE DCC DEVICE.

the PAM, the effect on overall force output and contraction was assumed to be negligible.

Force, Contraction, and Rise Time Requirements

The force requirements of the actuators for the DCC device can be estimated using a simple model of a hemispherical DCC device cupped around the bottom of a spherical heart as shown in Fig. 2. In this simple, idealized model, the force from the PAM creates the tension, *T*. The free body diagram of a cross section passing through the center of the model DCC device is also shown in Fig 2. If the device and the heart are in equilibrium, the tension required to apply the pressure P_{assist} to the heart is

$$T = \frac{P_{assist} \cdot A_x}{2}, \tag{4}$$

where A_x is the projected cross-sectional area of the device. In a study using a cup-shaped pneumatic DCC device similar to the idealized model in Fig.2, an assistance pressure of 140mmHg (18.7kPa) was needed to restore pumping function to a totally arrested (no native cardiac function) canine heart [18]. Using the above hemispherical cup model and assuming a diameter equal to a typical transverse heart diameter in adult males (13cm)[19], this pressure would correspond to a required tensile force of approximately 60N. Alternatively, in cases where native cardiac function is impaired but not totally stopped, lower assistance pressures are required to raise cardiac output to normal levels. For example, an assistance pressure of 20mmHg (2.7kPa) applied using a cup-shaped assist device has been shown to significantly increase the ejection fraction of failing hearts in live sheep [20]. This assistance pressure roughly corresponds to a tension of only 10N using Eqn 5. These first order estimates suggest that a tension roughly in the range of 10N to 60N is suitable for DCC. In the envisioned DCC device, the total wall tension would be produced by multiple PAMs placed in the wall of the device in a transverse orientation. Actuation with more PAMs in parallel allows the force to be more distributed and perhaps gentler on the heart. To enable the use of more actuators in parallel, the diameter of the actuators was designed to be as small as was feasible with the fabrication techniques available.

Required contraction can be estimated using the measure of cardiac function called fractional shortening (FS). FS is a measure of the percent change in the length of a cardiac dimension between diastole (expansion) and systole (contraction). In cases of left ventricular dysfunction, FS is less than or equal to 25% [21]. The actuators developed here must provide similar or better percent contraction to be useful in DCC.

The response time of a direct cardiac compression device must be similar to the contraction time of the human heart. Systole occurs in about 0.3 seconds in humans, so rise times much less than 0.3s are desired in order to keep pace with the heart. If the contraction time of a DCC device were much longer than systole, filling of the heart's ventricles, which occurs after systole, could be impeded [22].

FABRICATION OF PNEUMATIC ARTIFICIAL MUSCLES

The fabrication procedure for the PAMs consisted of molding elastomeric tubing, preparing a mesh, bonding the mesh to the tubing, and then sealing the ends. Elastomeric tubing was molded in house using a low stiffness elastomer (Shore OO-30, Ecoflex 00-30, Smooth-on, Inc.) or higher stiffness elastomer (Shore A-28, Elastosil M4601, Wacker Chemie AG). To create the tubing, the mixed prepolymer was poured into a plastic mold and degassed in a vacuum chamber at 10kPa absolute pressure for 10 minutes. Afterwards, the elastomer was cured for 1 hour in a pressure chamber heated to 60°C. A minimum outer diameter of 8mm and wall thickness of 2mm was chosen because molds for narrower tubing were difficult to fill using gravity alone.

Before being molded over the elastomeric tubing, the mesh was locally modified to resist expansion at its ends and to prevent fraying. This was achieved by locally heating the mesh (expandable sleeving, Techflex, Inc.) and increasing the braid angle. Figure 3a shows the process diagram. The mesh was placed over a steel rod for support and the region of the tube that was not being modified was covered with heat shrink to maintain the orientation of the fibers underneath (steps 1-2). The end of the mesh sleeve was held to the rod with a ring of heat shrink tubing to prevent fraying when the ends were heated and compressed (step 3). The exposed mesh sleeve was compressed by sliding the two heat shrink protected areas together and was heated with a hot air gun (step 4). When the exposed mesh was compressed, it bulged to a larger diameter, but collapsed back to the diameter of the rod when heated. After the new configuration was achieved, the fibers were allowed to cool to lock the new shape into place and the heat

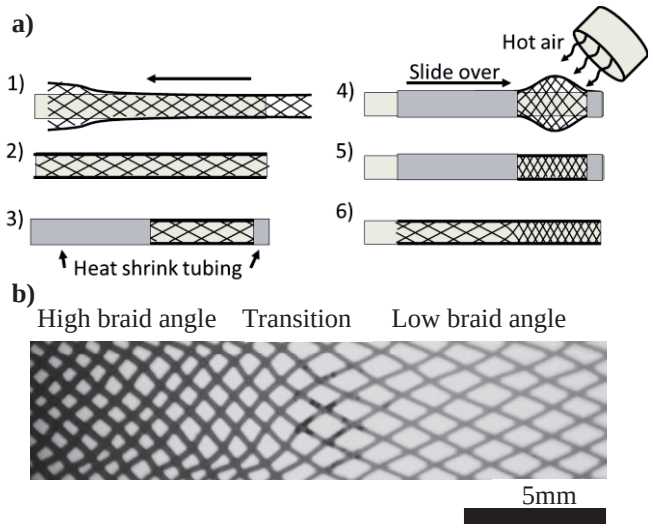

Figure 3. A) THE PROCESS DIAGRAM FOR VARYING THE MESH BRAID ANGLE. B) MICROSCOPE IMAGE OF A MODIFIED BRAID.

shrink was removed (steps 5-6). To verify that the braid angle was close to the neutral angle, manual expansion of the mesh was attempted and the resistance to expansion was assessed qualitatively. A mesh that was modified using the above procedure is shown in Fig. 3b.

Different initial mean braid angles were achieved by using different meshes between actuators or by using the same mesh and slightly changing the diameter of the actuator because diameter and braid angle are coupled. Since the braids were not made in-house, differences in mesh construction besides braid angle, like weave density, were not controlled for. The braid angle of each actuator was measured using a microscope (Table 1).

Table 1. BRAID MEASUREMENTS.

Mean θ_i (deg)	St Dev. (deg)	Initial diameter (mm)
22.6	0.8	8
28.6	0.7	8
31.7	1.1	8
39.5	1.6	10
45.1	0.5	12

Once the mesh was prepared, it was bonded to the outer wall of the elastomeric tube with another layer of elastomer. This was done by putting the mesh over the tube and dipping both into a basin of mixed prepolymer. When the tube was removed from the basin, the tube was blown with hot air while being rotated to evenly spread and cure the elastomer.

Finally, the ends of the actuator were closed by molding 2cm long elastomer plugs. The procedure for molding the plugs is shown in Fig. 4a. First, the tubing was put around a rod (step 1) and the tubing was extended past the end of the rod by 2cm and mixed prepolymer was poured into the tubing (step 2). The 2cm plug was cured at 60°C for one hour (steps 3-4). Next, an air supply line was inserted into the plugged end using a metal

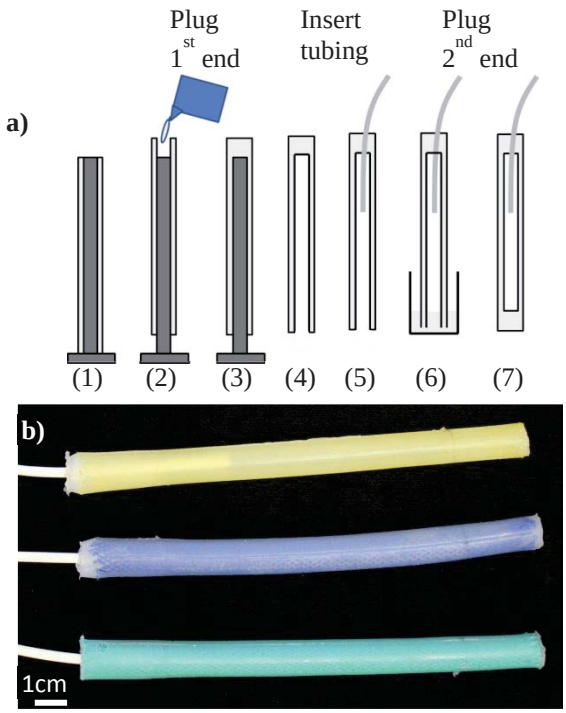

Figure 4. A) THE PROCEDURE FOR SEALING THE ENDS OF THE ACTUATOR. B) THE FINISHED ACTUATORS.

stylet (step 5). The remaining open end of the tube was dipped into a basin of mixed prepolymer to a depth of 2cm and cured at 60°C for 1 hour to form the second plug (step 6). During the dipping, the outer wall of the actuator was covered with PTFE tape to prevent the outer walls from bonding to the prepolymer in the basin. The finished actuators were 14cm long with a 10cm active length. The final outer diameter was about 8mm-14mm and the final wall thickness was about 1mm-2mm. Figure 4b shows some finished actuators.

EXPERIMENTAL CHARACTERIZATION

The actuators were characterized to determine whether they provided the appropriate force, contraction, and rise time for use in DCC. Isometric contraction tests were conducted to determine output force as a function of internal pressure while actuator length was held constant, and constant pressure contraction tests were conducted to measure force as a function of contraction while pressure was held constant. The isometric contraction test was conducted both quasi-statically and dynamically. Additionally, failure testing was conducted to determine the failure mode and pressure of the actuators.

For the isometric contraction test, the force output was measured using a 2 kN load cell (±4 N accuracy) and pressure was measured using a pressure transducer (±5 kPa accuracy) attached to the air supply line for the actuators. From these measurements, a force-pressure curve was generated. Figure 5a shows the test procedure. The pressure input was different in the quasi-static and dynamic testing. For the quasi-static

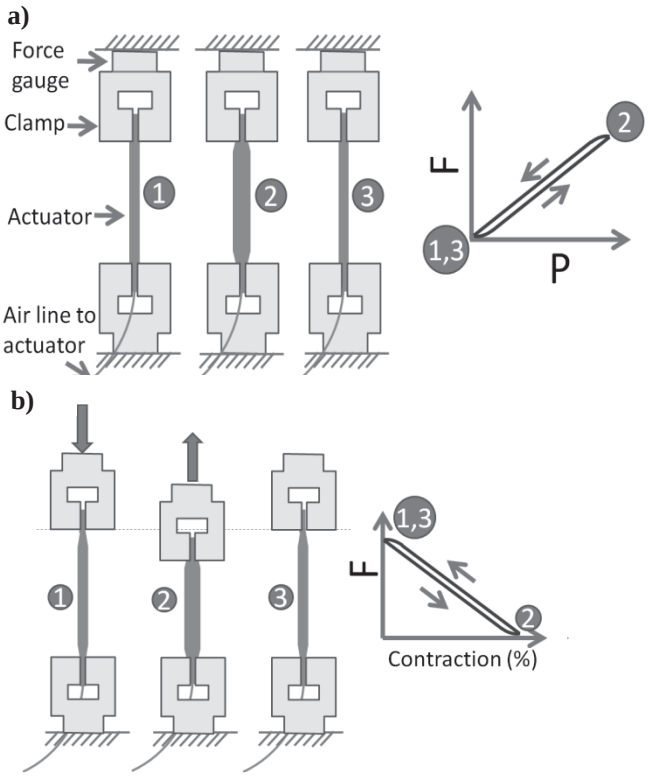

Figure 5. A SCHEMATIC OF THE TEST PROCEDURE FOR THE A) ISOMETRIC CONTRACTION TEST AND B) THE CONSTANT PRESSURE CONTRACTION TEST

response, the input pressure was slowly (T ≅ 60s) ramped from 0 to 103 kPa and back to 0 kPa using a pressure regulator. For the dynamic response a solenoid valve (2.4 mm orifice, 4-16 milliseconds response time) was used to quickly deliver air at 103 kPa from an accumulator (4.16L) to the actuators through about 1 m of tubing (ID = 3.2mm). A regulator was used to fill and continuously regulate the pressure in the accumulator.

For the constant pressure contraction test, the force and contraction were measured using a method previously used to characterize PAMs [23]. Figure 5b shows the experimental procedure. Tests were run at pressures of 34 kPa, 69 kPa, and 103 kPa, and an accumulator (4.16 L) was again used to maintain constant pressure. The contraction was varied by moving the actuator ends while the reaction force at the supports was measured. The actuator was allowed to contract until no load was measured at the supports (the "maximum contraction") and was then stretched back to the original length. Percent contraction was calculated by dividing displacement by the initial active length (10 cm). The contraction frequency was near physiological rates. A normal resting heart rate ranges from about 0.7 Hz-1.3 Hz, whereas the actuators were tested at ram speeds consistent with about 0.5 Hz contraction frequency.

Failure testing was also performed on the actuators. Pressure was delivered to each actuator using its air supply line and was slowly increased until failure. The tests were conducted with no load attached to the actuator. A pressure

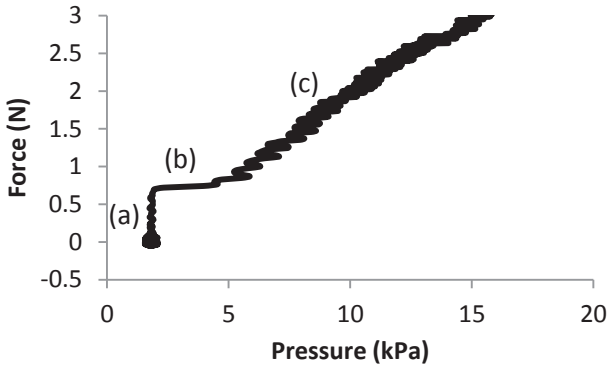

Figure 6. A TYPICAL FORCE VS PRESSURE CURVE FOR THE PNEUMATIC ARTIFICIAL MUSCLES AT LOW PRESSURE

sensor (accuracy: ±5 kPa) was used to measure the pressure during the test. The tests were filmed with a pressure sensor next to the muscle to enable confirmation of the pressure at the onset of failure.

Isometric Contraction Test Results

The force-pressure curves from the quasi-static isometric contraction test were used to measure the threshold pressure of the actuators and to examine the effects of initial mean braid angle and elastomeric material on the force output as a function of pressure. The low pressure region of the force-pressure curves was used to attempt to identify a threshold pressure. A typical force-pressure curve at low pressures is shown in Fig. 6. As the figure shows, the force-pressure curve is vertical in region (a) because an increase in force was measured before an increase in pressure was measured. In region (b), the pressure increase is detected and the pressure appears to increase without much change in force. After a pressure of about 5-7 kPa, the measured force increases linearly with measured pressure (region (c)). This pattern was nearly identical across all actuators. Region (a) is clearly an artifact because force cannot be developed by the actuators without pressure. Since the force increase was detected before any pressure, no pressure threshold could be detected for any of the actuators, but factoring in the accuracy of the sensor (±5 kPa), the threshold pressure of the actuators can be said to be below 5 kPa. This threshold pressure is an order of magnitude lower than those of McKibben air muscles tested in the literature [1,24].

In addition to identifying the threshold pressure, the effect of the elastomeric material on force output was assessed by comparing the force-pressure curves of two actuators that differed only in elastomeric material. The curves of the actuators made from low stiffness (Ecoflex OO-30) and high stiffness (Elastosil M4601) elastomer are shown in Fig. 7a. The slopes of the curves were similar between the muscles; the low stiffness actuator has a slope only 4% greater than the high stiffness actuator. The similarity between the curves was expected because deformation was prevented in this test, so

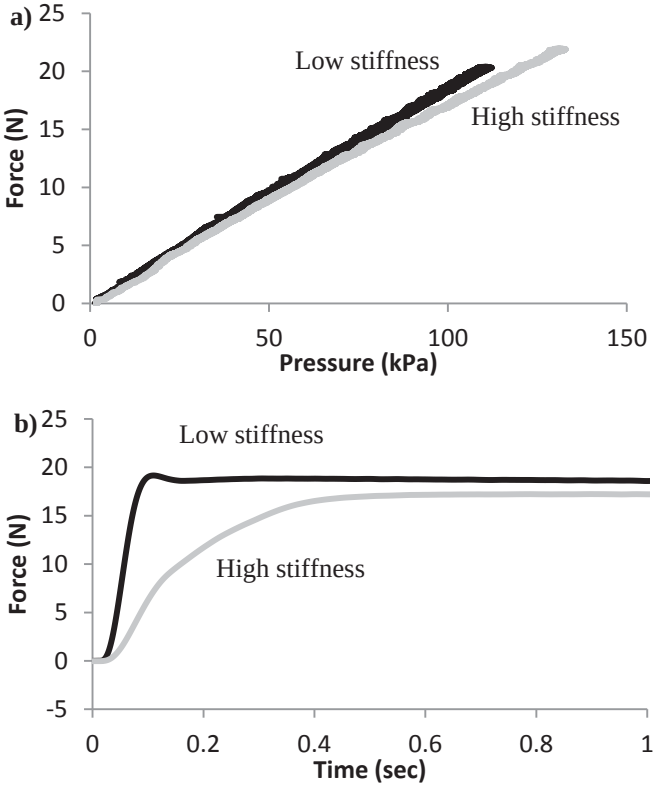

Figure 7. ISOMETRIC CONTRACTION CURVES FOR ACTUATORS MADE WITH ELASTOMERS OF DIFFERENT STIFFNESS. A) QUASISTATIC TEST RESULTS. B) DYNAMIC TEST RESULTS.

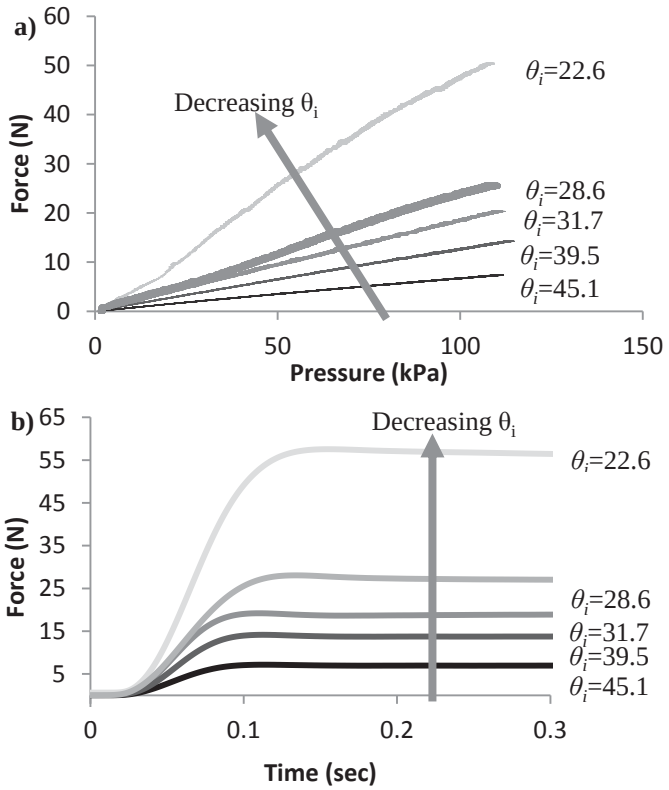

Figure 8. ISOMETRIC CONTRACTION CURVES FOR ACTUATORS WITH DIFFERENT INITIAL BRAID ANGLES. QUASISTATIC (A) AND DYNAMIC (B) TEST RESULTS.

almost no energy went to deforming the elastomer and therefore the different elasticities had little effect.

The dynamic responses of the two actuators are compared in Fig. 7b. The actuator made of the stiffer elastomer had a much longer rise time (0.28 s vs. 0.05 s). Based on the requirement of a rise time much less than 0.3 seconds, the actuator made of the softer elastomer contracted at a rate suitable for direct cardiac compression, but the actuator made of the stiffer elastomer did not.

The force-pressure curves from the isometric contraction test were also used to investigate the effects of initial mean braid angle on force output. The force-pressure curves of five artificial muscles that differed in initial mean braid angle are shown in Fig. 8a. All of the actuators were made of the low stiffness elastomer. For the actuators with an increased initial diameter, the effect of an increased braid angle, which is decreasing force, dominated the effect of the increased diameter, which is increasing force. The slope of the force-pressure curve increased with decreasing initial mean braid angle, θ_i. All the actuators except the one with the highest θ_i were able to develop at least 10 N of force at 100 kPa. This is suitable for DCC because even a single actuator could deliver force in the desired 10-60 N range at pressures of 100 kPa.

The dynamic responses of the actuators are also compared in Fig. 8b. All the actuators had a rise time of approximately 0.05 s. This suggests that initial mean braid angle does not have a significant effect on rise time and that the contraction times are suitable for DCC according to our requirement.

Constant Pressure Contraction Results

The constant pressure test results were used to assess whether the actuators produced suitable contraction for DCC and to evaluate the effect of elastomeric material and initial mean braid angle on contraction. The effect of different elastomeric materials was measured by testing two actuators that differed in elastomer stiffness. Force-displacement curves of the actuators made of the low stiffness (Shore OO-30) and high stiffness (Shore A-28) elastomers are shown in Fig 9a. As predicted, the force decreased monotonically as contraction increased for both actuators. Also, the curves exhibited low hysteresis (~1 N high, and 1% wide) compared to other McKibben PAMs [24] possibly due to lower friction. The actuator made of the stiffer elastomer had a dramatically lower maximum contraction (10% vs 24%). Only the contraction of the low stiffness elastomer comes close to the functional requirement of roughly 25% contraction.

The force-displacement curves of five artificial muscles that differed in braid angle are shown in Fig. 9b. All of the curves shown in the figure were taken at a pressure of 69 kPa. Each of the curves is monotonically decreasing and roughly linear. Again, the hysteresis was small (~1N high and 1%

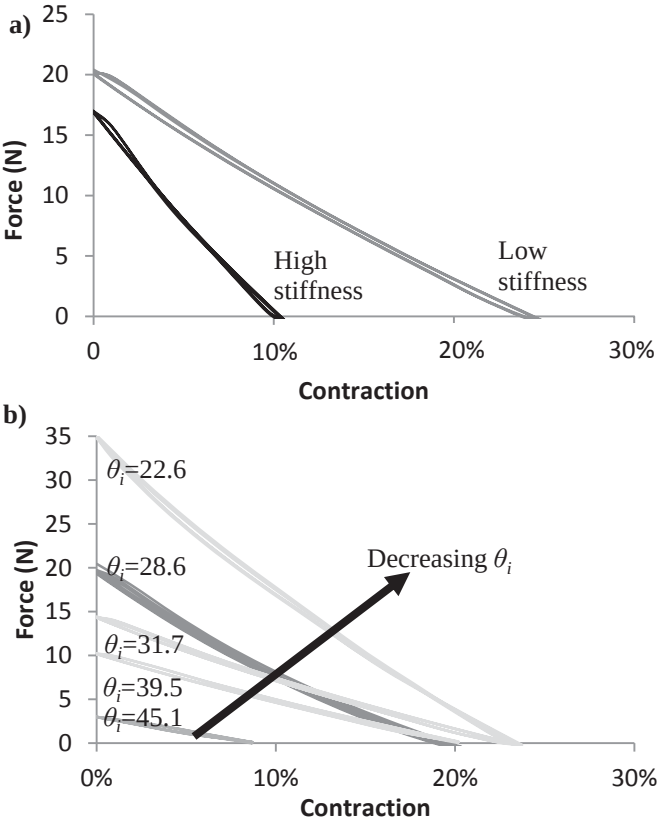

Figure 9. A) EFFECT OF ELASTOMERIC MATERIAL ON FORCE-CONTRACTION CURVE B) EFFECT OF INITIAL BRAID ANGLE ON FORCE-CONTRACTION CURVE .

wide). The maximum contraction and maximum force tended to increase with a decreasing initial mean braid angle, but it seems that the effect on maximum contraction was diminishing after θ_i=39.5°.

The actuator with θ_i=28.6° was an outlier because it had a lower maximum contraction than two actuators with a higher braid angle. This may be explained by the difference in mesh properties besides the braid angle, namely the weave density. Davis showed that higher fiber density caused a lower maximum contraction [25]. The two actuators with the lowest braid angle (θ_i=28.6°, θ_i=22.6°) had a higher weave density than the rest of the actuators, which had the same weave density.

In all of the actuators, a trade-off between force and contraction is apparent. It is difficult for the actuators to produce both high force and high contraction at once because force decreases with increasing contraction. However, force can be increased by adding more actuators in parallel which might enable more force to be sacrificed for contraction.

The actuators with lower initial mean braid angles were able to deliver greater force and contraction, so the most promising design seems to be one with the lowest possible initial mean braid angle. However, there is a lower limit to the initial mean braid angle because radial expansion increases with decreasing initial mean braid angle and space in the pleural cavity is limited. The actuators developed here undergo a diameter increase of about 1cm during contraction. This radial expansion is not considered to be large enough to be a problem for DCC, but in the future, the maximum allowable radial expansion should be determined to define the lowest feasible initial mean braid angle.

Failure Test Results

The first failure mode of the actuators made of the less stiff elastomer was that the air supply line slipped out. The line was ejected at 138 kPa – 228 kPa for three specimens made of the softer elastomer (Ecoflex OO-30). The air supply line was not ejected for the four actuators made of high stiffness elastomer (Wacker M4601), but the plug opposite the air supply line failed. Failure occurred at 270 kPa, 600 kPa, and 720 kPa. All of these ruptures pressures are significantly higher than the operating pressure of 100 kPa. In the future, a hybrid actuator that is mostly soft but has a stiffer elastomer where the air supply line is connected may prevent the disconnection of the line and raise the failure pressure of the soft actuators. The variation in rupture pressure was high, especially for the stiffer actuators, so testing of a larger sample size is needed to identify the factors that cause this variation.

CONCLUSION

Our experimental data showed that the fully soft pneumatic artificial muscles (PAMs) developed here have the ability to deliver suitable forces, contractions, and rise times for direct cardiac compression (DCC) in the pressure range of 0-100kPa. The actuators developed here also have threshold pressures significantly lower than traditional McKibben PAMs [1] which enables more precise control of force and displacement at low pressures.

The experimental results indicate that elastomeric material and initial mean braid angle greatly affect performance of the actuators. A softer elastomer enabled greater contraction and a much faster response time while a lower initial mean braid angle increased force output and maximum contraction. These results suggest that a DCC device powered by these actuators is feasible. The next step in the development of such a device is integrating the actuators into a soft, elastomeric structure that can be placed around the heart.

ACKNOWLEDGMENTS

We would like to acknowledge the Wyss Institute for Biologically Inspired Engineering for funding this research and Ramses Martinez, Michael Wehner, and Kevin Galloway for providing input on fabrication methods for soft actuators and methods for their experimental characterization.

REFERENCES

[1] Daerden F., and Lefeber D., 2002, "Pneumatic artificial muscles: actuators for robotics and automation," European Journal of Mechanical and Environmental Engineering.

[2] Andrikopoulos G., Nikolakopoulos G., and Manesis S., 2011, "A Survey on Applications of Pneumatic Artificial Muscles," Proceeding of the 10th Mediterranean Conference on Control Automation (MED), pp. 1439–1446.

[3] Oz M. C., Artrip J. H., and Burkhoff D., 2002, "Direct cardiac compression devices.," The Journal of Heart and Lung Transplantation, **21**(10), pp. 1049–55.

[4] Shahinpoor M., and Kim K., 2001, "Design, development, and testing of a multifingered heart compression/assist device equipped with IPMC artificial muscles," SPIE's 8th Annual International Symposium on Smart Structures and Materials, **4329**, pp. 411–420.

[5] Shahinpoor M., 2010, "A Review of Patents on Implantable Heart-Compression / Assist Devices and Systems," Recent Patents on Biomedical Engineering, pp. 54–71.

[6] Kung R. T., and Rosenberg M., 1999, "Heart booster: a pericardial support device.," The Annals of Thoracic Surgery, **68**(2), pp. 764–7.

[7] Moreno M. R., Biswas S., Harrison L. D., Pernelle G., Miller M. W., Fossum T. W., Nelson D. A., and Criscione J. C., 2011, "Assessment of Minimally Invasive Device That Provides Simultaneous Adjustable Cardiac Support and Active Synchronous Assist in an Acute Heart Failure Model," J. Med. Devices, **5**(4), p. 041008.

[8] Moreno M. R., Biswas S., Harrison L. D., Pernelle G., Miller M. W., Fossum T. W., Nelson D. a., and Criscione J. C., 2011, "Development of a Non-Blood Contacting Cardiac Assist and Support Device: An In Vivo Proof of Concept Study," J. Med. Devices, **5**(4), p. 041007.

[9] Trumble D. R., Park C. S., and Magovern J. a., 1999, "Copulsation Balloon for Right Ventricular Assistance : Preliminary Trials," Circulation, **99**(21), pp. 2815–2818.

[10] Shiraishi Y., Yambe T., Sekine K., Saijo Y., Wang Q., and Liu H., 2005, "Development of an Artificial Myocardium using a Covalent Shape-memory Alloy Fiber and its Cardiovascular Diagnostic Response.," Proceedings of the 27th Annual Conference of the IEEE Engineering in Medicine and Biology, **1**, pp. 406–8.

[11] Ming Y., Meiling Z., Richardson R. C., Levesley M. C., Walker P. G., and Watterson K., 2005, "Design and evaluation of linear ultrasonic motors for a cardiac compression assist device," Sensors and Actuators A: Physical, **119**(1), pp. 214–220.

[12] Klute G. K., Czerniecki J. M., and Hannaford B., 1999, "McKibben artificial muscles: pneumatic actuators with biomechanical intelligence," 1999 IEEE/ASME International Conference on Advanced Intelligent Mechatronics, pp. 221–226.

[13] Chou C., and Hannaford B., 1994, "Static and dynamic characteristics of McKibben pneumatic artificial muscles," IEEE Conference on Robotics and Automation.

[14] Woods B. K., Gentry M. F., Kothera C. S., and Wereley N. M., 2012, "Fatigue life testing of swaged pneumatic artificial muscles as actuators for aerospace applications," Journal of Intelligent Material Systems and Structures, **23**(3), pp. 327–343.

[15] Schulte H., 1961, "The characteristics of the McKibben artificial muscle," The Application of External Power in Prosthetics and Orthotics, pp. 94–115.

[16] Tondu B., 2012, "Modelling of the McKibben artificial muscle: A review," Journal of Intelligent Material Systems and Structures, **23**(3), pp. 225–253.

[17] Horn B., and Kuipers M., 1988, "Strength and stiffness of a reinforced flexible hose," Applied scientific research, **281**, pp. 251–281.

[18] Anstadt M. P., Perez-Tamayo R. a, Banit D. M., Walthall H. P., Cothran R. L., Abdel-Aleem S., Anstadt G. L., Jones P. L., and Lowe J. E., "Myocardial tolerance to mechanical actuation is affected by biomaterial characteristics.," ASAIO Journal, **40**(3), pp. M329–34.

[19] Oberman a., Myers a. R., Karunas T. M., and Epstein F. H., 1967, "Heart Size of Adults in a Natural Population-Tecumseh, Michigan: Variation by Sex, Age, Height, and Weight," Circulation, **35**(4), pp. 724–733.

[20] Carrington R., and Huang Y., 2003, "Direct compression of the failing heart reestablishes maximal mechanical efficiency," The Annals of Thoracic Surgery, pp. 190–196.

[21] Mosterd a, Hoes a W., De Bruyne M. C., Deckers J. W., Linker D. T., Hofman A., and Grobbee D. E., 1999, "Prevalence of heart failure and left ventricular dysfunction in the general population; The Rotterdam Study.," European Heart Journal, **20**(6), pp. 447–55.

[22] Walker P. G., Keeling D. G., Levesley M. C., Hanson B., Watterson K., and Ipereni C., "Do We Need Active Relaxation in Artificial Cardiac Muscles?," Engineering In Medicine And Biology, **l**, pp. 2–4.

[23] Wehner M., Park Y.-L., Walsh C., Nagpal R., Wood R. J., Moore T., and Goldfield E., 2012, "Experimental characterization of components for active soft orthotics," Proc. IEEE Int. Conf. Biomed. Rob. Biomechatron., pp. 1586–1592.

[24] Chou C., and Hannaford B., 1996, "Measurement and modeling of McKibben pneumatic artificial muscles," IEEE Conference on Robotics and Automation, **12**(1), pp. 90–102.

[25] Davis S., 2006, "Braid Effects on Contractile Range and Friction Modeling in Pneumatic Muscle Actuators," The International Journal of Robotics Research, **25**(4), pp. 359–369.